Table 1. Purification of bursin from the chicken bursa of Fabricius.

Purification step	Total bursin (mg)	Total protein (mg)	Bursin (%)	Purification (fold)	Recovery (%)
Chicken bursa (wet weight, 180 g)	6.5	7986	0.08	1	100
Gel filtration, Sephadex G-50	2.9	25.5	11.4	142	45
Solvent partitioning, upper phase	1.54	1.87	82	1012	24
Crystallization	1.36	1.41	96.5	1185	21

Gly-NH_2), cAMP and cGMP were increased and the dose-response curves were similar (Fig. 3). The threshold concentrations were 0.1 to 1.0 μg/ml, with the maximal response at 100 μg/ml. The three control synthetic tripeptides increased cAMP and cGMP only at concentrations 1×10^3 to 1×10^4 higher than those for natural and synthetic bursin. Thymopentin did not increase cAMP or cGMP in Daudi cells but elevated cGMP in CEM T cells (*9*). Bursin did not affect cGMP in CEM or three other T-cell lines, the erythropoietic stem cell line K562, and five other B-cell lines, although it did increase cGMP in the murine B-cell line MOPC 315 (American Type Culture Collection TIB 23). Natural and synthetic bursin also induced selective phenotypic differentiation of murine precursor B cells but not precursor T cells, in conformity with previous avian and mammalian inductive studies with partially purified bursal extracts (*6, 7*). Thus bursin and thymopoietin display the reciprocal inductive selectivity for B versus T cells that seems appropriate to physiological inducers for these two cell lineages. Furthermore, preliminary immunohistological studies in the chicken with antibodies to bursin indicate that bursin production is restricted to the bursa of Fabricius.

Gly-His-Lys has been detected in extracts of rat liver and is reported to be a growth factor (*10*). The activity of this tripeptide and of Gly-His-Lys-NH_2 and Lys-His-Gly in the bursin assays is provocative and may imply a tertiary structure distantly resembling that of bursin, but the weak inductive capacity, 1×10^3 to 1×10^4 lower than that of bursin, suggests that this activity is physiologically irrelevant.

We conclude that the structure of chicken bursin is Lys-His-Gly-NH_2 and that this tripeptide avian hormone has similar actions in birds and mammals, including humans. The presence of receptors for avian bursin on murine and human cells would suggest that the tripeptide structure of bursin has been conserved in evolution, but the occurrence and structure of the mammalian equivalent of bursin and its site of production remain to be determined.

REFERENCES AND NOTES

1. G. Goldstein, *Nature (London)* **247**, 11 (1974); R. S. Basch and G. Goldstein, *Proc. Natl. Acad. Sci. U.S.A.* **71**, 1474 (1974); D. H. Schlesinger and G. Goldstein, *Cell* **5**, 361 (1975).
2. M. P. Scheid, G. Goldstein, E. A. Boyse, *J. Exp. Med.* **147**, 1727 (1978).
3. G. H. Sunshine *et al.*, *J. Immunol.* **120**, 1594 (1978); T. Audhya, M. A. Talle, G. Goldstein, *Arch. Biochem. Biophys.* **234**, 167 (1984).
4. G. Goldstein, M. P. Scheid, E. A. Boyse, D. H. Schlesinger, J. Van Wauwe, *Science* **204**, 1309 (1979).
5. B. Glick, T. S. Chang, R. G. Jaap, *Poult. Sci.* **35**, 224 (1956); M. D. Cooper, R. Peterson, M. A. South, R. A. Good, *J. Exp. Med.* **123**, 75 (1966).
6. A. Brand, D. G. Gilmour, G. Goldstein, *Science* **193**, 319 (1976).
7. G. Goldstein *et al.*, *Cold Spring Harbor Symp. Quant. Biol.* **41**, 5 (1977).
8. D. H. Spackman, W. H. Stein, S. Moore, *Anal. Chem.* **30**, 1190 (1958).
9. T. Audhya, M. A. Talle, G. Goldstein, *Arch. Biochem. Biophys.* **234**, 167 (1984).
10. L. Pickart and M. M. Thaler, *Nature (London) New Biol.* **243**, 85 (1973).
11. A. L. Steiner *et al.*, *J. Biol. Chem.* **247**, 1106 (1972).

12. We thank M. Scheid for performing bursin induction assays with murine cells and J. Lloyd for mass spectroscopy. We also thank R. King, B. Baker, H. Dreskin, J. Chen, J. Perry, R. Sulsky for technical assistance; N. Lawery for typing; and M. Gardner for editing.

4 June 1985; accepted 21 November 1985

Hyperacuity in Cat Retinal Ganglion Cells

ROBERT SHAPLEY AND JONATHAN VICTOR

Cat X retinal ganglion cells that can resolve sine gratings of only 2.5 cycles per degree can nevertheless respond reliably to displacements of a grating of approximately 1 minute of arc. This is a form of hyperacuity comparable in magnitude to that seen in human vision. A theoretical analysis of this form of hyperacuity reveals it to be a result of the high gain and low noise of ganglion cells. The hyperacuity expected for the best retinal ganglion cells is substantially better than that observed in behavioral experiments. Thus the brain, rather than improving on the retinal signal-to-noise ratio by pooling signals from many ganglion cells, is unable to make use of all the hyperacuity information present in single ganglion cell responses.

HUMAN OBSERVERS CAN DETECT the change in position of a grating when the displacement is only 10 seconds of arc, which is the visual angle subtended by 1 cm at a distance of 200 m. In other spatial localization tasks, the threshold for displacement is also a small fraction of the interreceptor spacing in the fovea (equivalent to about 30 seconds). Such performance, in which the threshold for detecting positional displacements is much smaller than the inverse of the spatial frequency resolution, has been called hyperacuity (*1*). We have studied spatial localization acuity of cat retinal ganglion cells and found that single X ganglion cells (*2*) can respond reliably to displacements more than an order of magnitude smaller than the radius of the receptive field center. This retinal hyperacuity is a consequence of the high gain and low noise of the receptive field center mechanism.

Visual stimuli were produced on a Tektronix 608 CRT monitor with a raster display by means of an electronic display instrument (*3*). A computer sent control signals to the instrument and measured the times when nerve impulses occurred. The stimuli were spatial sine gratings on a mean luminance of 140 cd/m². In the grating displacement experiments, spatial phase of the grating was shifted back and forth a fixed displacement every 474 msec; the displacement was repeated 64 times and the displacement responses averaged. In these displacement experiments, the contrast of the grating—$(L_{max} - L_{min})/(L_{max} + L_{min})$—was held constant at 0.5. In other experiments gratings were not displaced; instead, the contrast of stationary gratings was varied sinusoidally in time at a frequency of approximately 1 Hz. Responses to 32 cycles of modulation were averaged in these runs. Single-unit recordings of optic tract fibers were obtained with Ringer-filled glass micropipettes. Details of our procedure for recording from anesthetized and paralyzed cats are given in (*4*). Ganglion cells were classified as X or Y on the basis of a modified null test (*2*).

R. Shapley, Rockefeller University, New York, NY 10021.
J. Victor, Rockefeller University, and Cornell University Medical College, New York, NY 10021.

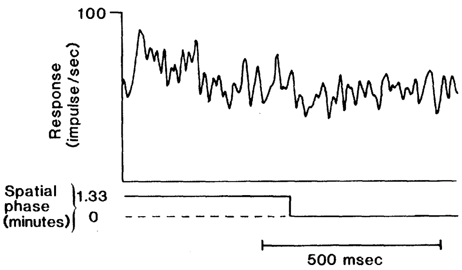

Fig. 1. Response of a cat retinal ganglion cell to abrupt 1.3-minute displacements about the null of an 0.8 cycle/deg grating at a contrast of 0.5. The histogram has been smoothed by digital convolution with a bell of half-width 6 msec. Unit 12/1, on-center X cell.

Retinal ganglion cells can respond reliably to very small displacements. We measured such responses in three near-peripheral on-center X cells. The largest responses to displacement were produced when the sine grating stimulus was placed at the null position, the spatial phase of the grating at which no response is produced by contrast modulation (*2*). The response of one of the cells to a 1.3-minute displacement is shown in Fig. 1. The height of the transient response was approximately 20 impulses per second; it was clearly detectable by the experimenters on an audio monitor. The spatial frequency resolution of this cell was about 2 cycle/deg (Fig. 2). A summary of the data from all three cells is presented in Table 1. Although none of the units resolved a grating of spatial frequency higher than 2 cycle/deg, all had large responses to grating displacements of less than 3 minutes. The response to a given displacement was larger at a spatial frequency well below the high frequency cutoff of the cell than at a just-resolvable spatial frequency.

For small displacements about the null spatial phase, the response was approximately proportional to displacement as shown in Fig. 3. For small displacements about the peak spatial phase, which is the position at which the grating produces the largest response to contrast modulation, the response grew proportionally to the square of the displacement and was not out of the noise until the displacements were larger than 10 minutes (Fig. 3). From spatial frequency responses (Fig. 2), one could estimate the radii of the receptive field centers to be in the range of 15 to 25 minutes.

Although the averaged response amplitudes were larger than noise for small grating displacements, one would like to know whether individual displacements would have been detectable on the basis of the ganglion cells' responses. One approach to this problem is to estimate the signal-to-noise (S:N) ratio of the filtered impulse train (*5*). An approximation to optimal filtering is a low-pass filter with an integration time equal to that of the photoreceptors, about 40 msec (*6*). With such filtering, the S:N ratio in an averaged response to a grating displacement of 1.3 minute (Fig. 1) was about 10:1. Since S:N ratio increases with the square root of the number of cycles averaged, such an S:N ratio from the average response to 64 grating displacements is equivalent to an S:N ratio of 1.25:1 for a single displacement. If we assume that reliable detection requires an S:N of 2:1, the displacement acuity limit for the retinal ganglion cell that generated Fig. 1 was (1.3 minutes) × (2/1.25) = 2.1 minutes. These experiments were done with 0.5 contrast; under the assumption of linearity, the displacement threshold of a unity contrast grating would be halved to about 1 minute. This is not the ultimate in cat retinal ganglion cell hyperacuity. On a theoretical basis, we predict that retinal ganglion cells in the cat's area centralis should respond reliably to 10-second displacements.

Let us analyze the relation between displacement acuity and spatial frequency resolution in terms of a linear model of the receptive field. The assumption of linearity is an approximation; any saturation of response at high contrast would increase the displacement threshold to values higher than predicted from this approximation. The agreement of data and predictions in Fig. 3 is evidence that linearity is a good approximation. For ease of calculation we assume even symmetry and ignore the effects of response dynamics (*7*).

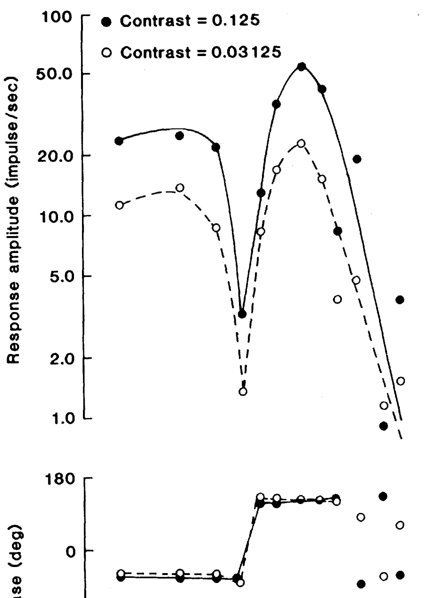

Fig. 2. Responses to standing, sinusoidally modulated gratings positioned in peak spatial phase of contrast 0.125 (filled symbols) and 0.03 (open symbols). At spatial frequencies below 0.4 cycle/deg, the surround response is dominant and phase has shifted by 180°. This strong surround does not affect the measurements of spatial frequency resolution or grating displacement resolution, which were all done at high spatial frequencies for which the surround contribution to the cell's response was negligible. Unit 12/1, on-center X retinal ganglion cell.

Table 1. Responses (impulses per second) of three on-center X ganglion cells to grating displacements.

Spatial frequency (cycle/deg)	Responses at a grating displacement of 2.34 min	4.68 min	9.37 min
	Unit 10/11—eccentricity 3.5°		
0.8	17.5	28.2	37.8
1.6	8.1	10.8	24.5
	Unit 11/8—eccentricity 6.0°		
0.8	11.9	22.5	34.4
	Unit 12/1—eccentricity 3.2°		
0.8	8.4	17.0	29.9
1.6	4.1	6.3	11.4

Assume that the receptive field center has a linespread function equal to a product of a contrast gain A (in units of impulses per second per unit contrast) and a normalized linespread $g(x)$. We define a normalized spatial frequency response $G(k)$ to be the Fourier transform of $g(x)$ (*8*). Let b be a threshold criterion equal to two standard deviations of the impulse rate variability in impulses per second. A reasonable value for b inferred from our data is 40 impulses [compare with (*5*)]. Grating contrast is denoted c.

We call the dimensionless combination cA/b the parameter Z. Z is proportional to the optimal (across all stimuli) signal-to-noise ratio because it is the ratio of the maximum response, cA, to b, the measure of impulse rate variability. In the present analysis, c is 0.5, b is 40 impulse sec, and A is in the range 800 to 1600 impulse sec per unit contrast for transient responses (*6*). Thus, Z is in the range 10 to 20; we assume an average value of 15 in what follows.

The maximal response to contrast modulation of a sine grating of spatial frequency k is $cAG(k)$. At the spatial resolution limit, $cAG(k_{\text{resol}}) = b$, and therefore the highest spatial frequency resolvable k_{resol} is implicitly defined by the equation:

$$G(k_{\text{resol}}) = \frac{b}{cA} = \frac{1}{Z} \tag{1a}$$

and therefore,

$$k_{\text{resol}} = G_{\text{inv}}\,(1/Z). \tag{1b}$$

Next, we calculate $R_D(k,\Delta x)$, the response to a displacement of a grating of spatial frequency k by an amount Δx. This response depends on the initial phase of the grating. One can show that, at the null position, R_D is proportional to displacement (*9*) as in Fig. 3:

$$R_D(k,\Delta x) = 2\pi cAG(k)k\Delta x \qquad (2)$$

Since in Eq. 2 the displacement response depends on $k\ G(k)$, the optimum spatial frequency for detecting a displacement, k_D, can be calculated by finding the spatial frequency that produces the maximum $k\ G(k)$.

At displacement threshold, the displacement response just equals the detection criterion b. Thus, $R_D(k_D, \Delta x_D) = b$. Using Eq. 2, one calculates the threshold displacement, Δx_D:

$$\Delta x_D = \frac{1}{2\pi Z\ k_D\ G(k_D)} \qquad (3)$$

A measure of hyperacuity is the ratio of $1/k_{resol}$ to Δx_D, which is (from Eqs. 1a, 1b, and 3):

$$\frac{1}{k_{resol} \cdot \Delta x_D} = \frac{2\pi Z\ k_D G(k_D)}{G_{inv}\ (1/Z)} \qquad (4)$$

This general result demonstrates the dependence of hyperacuity on Z, the signal-to-noise ratio. From Eq. 3, the displacement threshold is inversely proportional to Z. If the linespread function $g(x)$ is smooth, the spatial frequency resolution, k_{resol}, equal to $G_{inv}(1/Z)$ from Eq. 1b, is a shallow function of Z (*10*). Therefore, as Z grows large, the measure of hyperacuity in Eq. 4, which involves a ratio of Z to a shallow function of Z, grows without bound. Equation 4 thus demonstrates the direct link beween hyperacuity and a large signal-to-noise ratio, Z.

As an example, consider a Gaussian receptive field with effective radius r and a linespread function:

$$g_{Gauss}(x) = \frac{1}{\sqrt{\pi}\ r} \exp\ (-x^2/r^2) \qquad (5)$$

and a corresponding spatial frequency response

$$G_{Gauss}\ (k) = \exp(-\pi^2k^2r^2) \qquad (6)$$

Using Eqs. 1a and 1b and a value of 15 for Z, one calculates

$$\frac{1}{k_{resol}} = \frac{\pi r}{[\log(Z)]^{1/2}} = 1.91r \qquad (7)$$

The optimum spatial frequency for detecting displacement, k_D, is equal to $1/\sqrt{2}\pi r$ (*11*). From Eq. 3, the displacement acuity is then:

$$\Delta x_D = \frac{r\sqrt{e}}{Z\sqrt{2}} = 0.078r \qquad (8)$$

Thus, for a Gaussian linespread, displacement acuity is about 24 times that of the inverse of spatial frequency resolution. This analysis of Gaussian linespread hyperacuity accounts for our experimental observations quantitatively. For the ganglion cell in Fig. 1, the value of k_{resol} was 2 cycle/deg, and therefore the predicted Δx_D according to Eq. 8 is 1.2 minute, in good agreement with experimental results. The presence of an inhibitory surround does not alter this result. If the inhibitory surround is as usual large in comparison with the center (*4, 7*), the surround response will be negligible at the relevant spatial frequencies k_D and k_{resol}.

The experimental and theoretical results reported here are significant for our understanding of hyperacuity. Recently it was found that cats have a behavioral displacement threshold of about 1 minute (*12*). This is larger than we predict for the best central ganglion cells, and is close to Δx_D for the peripherally located ganglion cells reported here. According to our analysis and the known properties of primate ganglion cells (*13, 14*), one should expect retinal hyperacuity in humans to be less than 4 seconds, while behavioral hyperacuity is around 10 seconds. Recent calculations of displacement resolution from spatial frequency resolution for monkey striate cortical neurons have reached the same values (*15*). This similarity implies that grating displacement hyperacuity is achieved first in the retina. Of course, not all hyperacuity performance can be a result simply of linear spatial filtering by the retina. There are examples of hyperacute binocular spatial localization (*1, 16*). However, our results suggest that before complex central processing is invoked to explain hyperacuity, one should check the consequences of linear filtering.

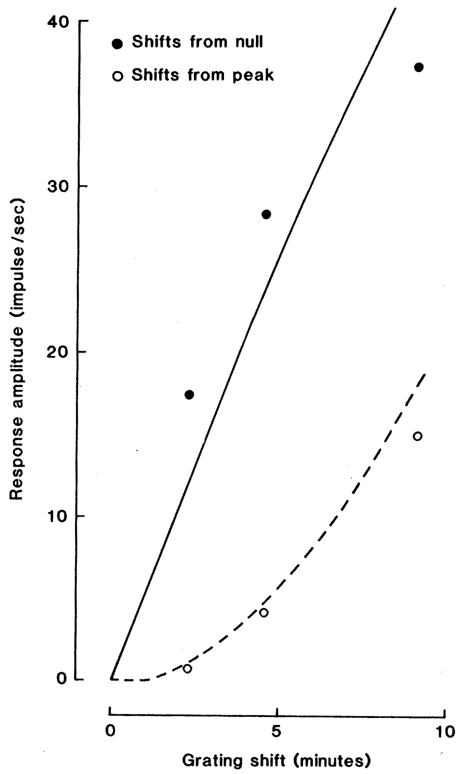

Fig. 3. Amplitude of fundamental component of response to abrupt displacements about the null (filled symbols) and the peak (open symbols) of an 0.8 cycle/deg grating at a contrast of 0.5. The curves are generated from Eq. 2 and (*9*) with a least-squares best fit value for A of 787 for the fundamental component. Unit 10/11, on-center X cell.

Our analysis shows that hyperacuity is a general property of ganglion cell receptive fields since Δx_D is much smaller than $1/k_{resol}$ even for large receptive fields, provided only that the linespread function is continuous (*10*). Previously it has been hypothesized that hyperacuity required perceptual interpolation in the brain to overcome the supposed lack of information in retinal neurons (*17*). However, our results imply that precise information about grating position is present in retinal ganglion cell impulse trains but is not used optimally by the brain. The brain's performance may be degraded by visual noise caused by eye movements or by other sources of internal noise such as fluctuations of selective attention. Whatever the causes, this hyperacuity does not reveal the prodigious information-processing capacity of the brain, but rather its limitations.

Note added in proof: While this report was in press, we learned about the recent psychophysical findings on displacement hyperacuity of Nakayama and Silverman (*18*), who found a significant response compression in the cortex's response to grating displacements—another reason, besides increased noise, why behavioral hyperacuity performance may be worse than predicted from retinal ganglion cell hyperacuity.

REFERENCES AND NOTES

1. G. Westheimer, *Invest. Ophthalmol.* **18**, 893 (1979).
2. C. Enroth-Cugell and J. G. Robson, *J. Physiol. (London)* **187**, 517 (1966); S. Hochstein and R. M. Shapley, *ibid.* **262**, 237 (1976).
3. N. Milkman *et al.*, *Behav. Res. Methods Instrum.* **12**, 283 (1980).
4. J. D. Victor and R. Shapley, *J. Gen. Physiol.* **74**, 275 (1979).
5. H. B. Barlow and W. R. Levick, *J. Physiol. (London)* **200**, 1 (1969); P. Lennie, *Vision Res.* **19**, 425 (1979).
6. R. M. Shapley and J. Victor, *J. Physiol. (London)* **318**, 161 (1981).
7. S. Dawis, R. Shapley, E. Kaplan, D. Tranchina, *Vision Res.* **24**, 549 (1984).
8. Thus,

$$G(k) = \int_{-\infty}^{\infty} dx\ \exp(-2\pi ikx)g(x)$$

9. The response of an X cell to a sine grating is a sinusoidal function of spatial phase (*2*). Thus, $R(k,\phi) = cAG(k)\ \cos(\phi)$ where ϕ is the spatial phase with the convention that $\phi = 0$ is the spatial phase of peak response and $\phi = \pi/2$ is the spatial phase of the null position. The response to a displacement Δx is the difference between the responses at spatial phase ϕ and spatial phase

$\phi + 2\pi k\Delta x$. Thus, $R_D = cAG(k)$ $[\cos(\phi) - \cos(\phi + 2\pi k\Delta x)]$. If $k\Delta x$ is small, then the expression in brackets may be represented as a Taylor series in powers of $k\Delta x$. The coefficient of the first term in the series involving $k\Delta x$ is $2\pi\sin(\phi)$, which has its maximal value at the null position where $\phi_n = \pi/2$ and $\sin(\phi_n) = 1$, and which goes to zero at the peak position where $\sin(p) = 0$. At the peak position, the first nonzero term in the Taylor expansion for R_D is $2\pi^2\ cAG(k)\ k^2\Delta x^2$. M. Sur and S. M. Sherman [*Exp. Brain Research* **56**, 497 (1984)] offered a similar analysis.
10. In general, smooth linespread functions $g(x)$ have Fourier transforms $G(k)$ that for large k are asymptotically bounded by k^{-p} (for $p > 1$) or e^{-k}, depending on the technical conditions used to define smoothness. If we assume $G(k)$ is equal to one or the other of these bounding functions, say $G(k) = k^{-p}$, or $G(k) = e^{-k}$, then, respectively, from Eq. 1a, $(k_{resol})^{-p} = 1/Z$ or, $\exp(-k_{resol}) = 1/Z$ implying that k_{resol} equals either $Z^{1/p}$ or $\log(Z)$. Since $G(k)$ is not equal to these functions of Z, but rather is bounded by them, we obtain the result that $k_{resol} = G_{inv}(1/Z)$ is asymptotically bounded by $Z^{1/p}$ or $\log Z$. Both of these rates of increase are substantially shallower than proportional to Z. A stronger result holds for the linespread functions of usual models (Gaussian, difference of Gaussians, Laplacian of Gaussians) and for any linespread function which takes convolution with optical blur into account. In these cases, k_{resol} is asymptotically proportional to $(\log Z)^{1/2}$. For the Gaussian linespread function, these asymptotic limits are reached even when Z is of order 3, well below the physiological range. Thus, $(\log Z)^{1/2}$ is a very good approximation for the dependence of spatial frequency resolution on signal-to-noise ratio.
11. The spatial frequency optimum for displacement, k_D, is calculated by maximizing the function $kG(k)$. This is done by finding the zeroes of the first derivative of $kG(k)$. Thus, for the Gaussian $[kG(k)]' = [1 - 2k^2\pi^2r^2]G(k) = 0$ at $k_D = 1/(\sqrt{2}\,\pi r)$.
12. D. E. Mitchell, personal communication.
13. C. B. Blakemore and F. Vital-Durand, *Trans. Ophthalmol. Soc. U.K.* **99**, 363 (1979); E. Kaplan and R. Shapley, *Invest. Ophthalmol. Suppl.* **25**, 120 (1984); A. M. Derrington and P. Lennie, *J. Physiol. (London)* **357**, 219 (1984).
14. From (*13*), the value of k_{resol} for foveal ganglion cells in monkeys is around 40 cycle/deg and the contrast gain A for the most sensitive monkey ganglion cells is the same as that of cat ganglion cells. Therefore, from Eqs. 6 and 7, one can estimate that the threshold for displacement should be $1/(k_{resol} \cdot 24)$, that is $1/(40 \cdot 24)$ degree, or approximately 4 seconds.
15. A. Parker and M. Hawken, *J. Opt. Soc. Am.* **2**, 1101 (1985).
16. M. J. Morgan and R. J. Watt, *Vision Res.* **22**, 863 (1982).
17. H. B. Barlow, *Proc. R. Soc. London Ser. B.* **212**, 1 (1981); F. H. C. Crick, D. C. Marr, T. Poggio, in *The Organization of the Cerebral Cortex*, F. O. Schmitt, F. G. Worden, G. Edelman, S. G. Dennis, Eds. (MIT Press, Cambridge, MA 1981).
18. K. Nakayama and G. H. Silverman, *J. Opt. Soc. Am.* **2**, 267 (1985).
19. Supported by National Eye Institute grants 2R01-EY 1472 and 1R01-EY 5466, by NINCDS grant NS 877, by the Air Force Office of Scientific Research grant 84-0278, and by the Hartford Foundation and the McKnight Foundation.

7 June 1985; accepted 25 October 1985

Gonadotroph-Specific Expression of Metallothionein Fusion Genes in Pituitaries of Transgenic Mice

Malcolm J. Low, Ronald M. Lechan, Robert E. Hammer, Ralph L. Brinster, Joel F. Habener, Gail Mandel, Richard H. Goodman

Transgenic mice expressing a metallothionein-somatostatin fusion gene contain high concentrations of somatostatin in the anterior pituitary gland, a tissue that does not normally produce somatostatin. Immunoreactive somatostatin within the anterior pituitaries was found exclusively within gonadotrophs. Similarly, a metallothionein–human growth-hormone fusion gene was also expressed selectively in gonadotrophs. It is proposed that sequences common to the two fusion genes are responsible for the gonadotroph-specific expression.

Foreign genes under the control of either their own or heterologous promoters are expressed in various tissues in transgenic mice. Expression of genes may be limited to specific tissues depending on the particular promoter, enhancer sequences, or undetermined elements (*1*). Several experiments involving transgenic mice have made use of fusion genes containing the mouse metallothionein I (MT) promoter (*2, 3*). Recently we have shown that a fusion gene (MT-SS) consisting of the MT promoter, the protein-coding region of rat pre-prosomatostatin (pre-proSS), and exon 5 plus the 3′ flanking region of the human growth-hormone (hGH) gene was actively expressed in the anterior pituitaries of transgenic mice (*4*). This tissue does not normally produce somatostatin. We report here the distribution of somatostatin-containing cells in the anterior pituitaries of these transgenic mice and show that expression is restricted to gonadotrophs. Additionally, we demonstrate that, in MT-hGH transgenic mice, expression of the fusion gene within the pituitary also occurs exclusively in gonadotrophs. We propose that the MT promoter, either alone or in concert with other sequences common to the two fusion genes, results in gonadotroph-specific expression.

Fusion genes containing the mouse MT promoter, rat pre-proSS complementary DNA or the hGH structural gene, and the hGH 3′ flanking region are depicted in Fig. 1. A portion of exon 5 and the 3′ flanking region of the hGH gene were retained in the somatostatin construction to provide polyadenylation and transcriptional termination signals. The fusion genes were microinjected into the male pronuclei of fertilized eggs from C57 × SJL hybrid mice, and the eggs were transplanted into the reproductive tracts of random-bred Swiss mouse foster mothers (*5*). Founder mice with integrated fusion genes were outbred to produce several pedigrees of heterozygous transgenic mice

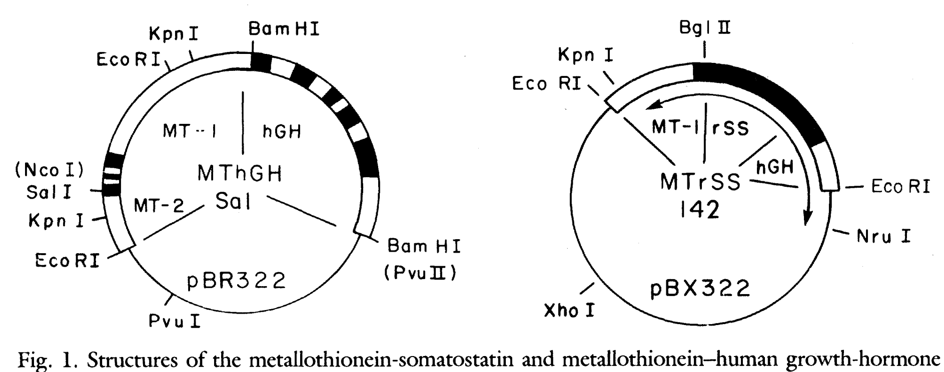

Fig. 1. Structures of the metallothionein-somatostatin and metallothionein–human growth-hormone fusion genes. The plasmid MTrSS 142 was constructed as described (*4*). MThGH Sal has an 8000-bp Kpn fragment of the mouse MT gene (*12*) inserted into MThGH 111 (*3*). Plasmid pBX322 or pBR322 sequences are denoted by a solid line, introns and flanking sequences by open boxes, and exons by closed boxes. The linearized fragment of MTrSS used for microinjection is indicated by a double-headed arrow. MThGH Sal was linearized at the Pvu I site. Both injected fragments contain portions of the MT-1 promoter and first exon (*12*) and portions of the hGH exon 5 and 3′ flanking regions (*13*). The two gene constructions differ in the structural coding sequences.

M. J. Low, R. M. Lechan, G. Mandel, R. H. Goodman, Division of Endocrinology, Tufts–New England Medical Center, Boston, MA 02111.
R. E. Hammer and R. L. Brinster, Laboratory of Reproductive Biology, School of Veterinary Medicine, University of Pennsylvania, Philadelphia 19104.
J. F. Habener, Laboratory of Molecular Endocrinology and Howard Hughes Medical Institute, Massachusetts General Hospital, Boston 02114.